

Gray Water Recovery System Model by Solar Photocatalysis with TiO₂ Nanoparticles for Crop Irrigation

Hipólito Carbajal-Morán^{1*}, Rosa H. Zárate-Quiñones², Javier F. Márquez-Camarena¹

¹ Universidad Nacional de Huancavelica, Facultad de Ingeniería Electrónica-Sistemas, Jr. La Mar N° 755, Pampas-Tayacaja, Huancavelica, Perú

² Universidad Nacional del Centro del Perú, Unidad de Postgrado de la Facultad de Ciencias Forestales y del Ambiente, Av. Mariscal Castilla N° 3909-4089, Huancayo, Perú

* Corresponding author's e-mail: hipolito.carbajal@unh.edu.pe

ABSTRACT

The objective of the study was to establish the configuration of the system model to allow the effective recovery of gray water by solar photocatalysis with TiO₂ nanoparticles for irrigation of crops. A programmable solar photoreactor based on an S7 1500 PLC and online measurement sensors were used as materials. The inductive method was used to analyze the samples and the deductive method to determine the water quality. The research design used was experimental based on the response surface methodology (MSR) with 20 experiments, 6 of which were central experiments and 6 were axial experiments; these experiments were carried out on sunny days. As a result of the research, a gray water recovery model was obtained, part of this being an electronic system with a programmable photocatalyst, which allowed the development of the experiments. It was concluded that with a solar UV index of 12.21, a dose of titanium dioxide (TiO₂) nanoparticles 1.973 g/L and with an exposure period of 60.041 minutes of the solar photocatalyst to UV radiation on sunny days, gray water was recovered in 90% with a confidence level of 95% and a significance $\alpha = 0.05$, which translates into excellent quality according to the water quality index established in Peru (ICA-PE).

Keywords: polluted water, solar radiation, nanoparticles, photocatalysis.

INTRODUCTION

The human activities require water, which is the pillar for the economic development and social welfare. On average, three thousand liters of water per person are required to generate the products necessary for daily nutrition [Casadei & Albert, 2016]. Although irrigation for agricultural purposes represents only 10% of the water used, this is the activity with the highest consumption of fresh water on the planet [UNESCO, 2006].

The use of gray water from homes in different domestic activities can be found worldwide [Silva et al., 2008]. Thus, in several countries of the world, grey water is used in the activities that do not require drinking quality water, for example, for evacuating the toilet, watering gardens and cleaning certain areas in homes; thus, the benefits in terms of saving water are achieved. According

to various investigations, water reuse leads to savings of between 30 and 50% in the consumption of drinking water in homes [Kamizoulis, 2008; Mohamed et al., 2013].

In Brisbane, Australia, an investigation was carried out in which a reduction between 30 and 50% was achieved in the consumption of drinking water, through the use of gray water in the irrigation of lawns and ornamental gardens. The main concern to implement the use of this type of water in garden irrigation, are the chemical compounds and microorganisms that could be harmful to health; therefore, primary and secondary treatment is necessary for the reuse of gray water in homes. This is possible, as long as the relevant safety measures are taken [Jeppesen, 1996].

In a study by Almomani et al. [2018] the potential of photocatalytic processes to remove emerging pollutants was evaluated. The analysis

of the performance indicator showed that the combination of the solar photocatalytic oxidation process with the application of ozone (O_3) significantly increased the removal capacity, with greater mineralization, reduced the chemical requirements and energy demand. It concluded that these oxidation processes with degradation capacity improve the water quality. Adrados et al. [2014] determined that the microbial community is the predominant community in domestic wastewater where gray water is immersed and when performing the conglomerate analysis of bacterial band patterns, it was shown that the structure is related to the design of the treatment system and the load of organic material.

In the work developed by Barwal et al. [2016], a biofilm reactor with a mobile platform was implemented coupled to a parabolic structure to obtain the maximum elimination of organic load and disinfection of microbes from the wastewater. The results obtained showed that it is possible to reduce the concentration time of the photocatalyst to 240 min of solar exposure. In addition, this process can offer a practical solution, free of chemical elements and economically viable, since solar energy is available on sunny days with solar irradiation of 400 to 700 W/m^2 and on cloudy days with solar irradiation of 170 to 250 W/m^2 , achieving water with a pH value of 7.6 and DQO of 69%.

Due to the high demand for water for crop irrigation in Peru, several studies were carried out, such as the one by Deza Martí et al. [2017] that experimentally evaluated the degradation of the Cibacron Navy H-2G blue dye through the photocatalytic action of industrial TiO_2 nanoparticles from the Spanish company Avanzare. The nanoparticles correspond to the anatase phase; they have an approximate size of 26.6 nm, measured with transmission electron microscopy (TEM). The photocatalytic degradation was evaluated based on the dose of the photocatalyst from 0.1 g to 1.0 g; varying the concentration of the dye from 20 ppm to 100 ppm; the pH being tested ranged from 2 to 10. With UV-Visible spectrophotometry, monitoring of photocatalytic degradation was carried out. The optimal results found were with the dose of TiO_2 equal to 0.6 g for a concentration of 20 ppm of the dye and with pH 4.0.

The gray water becomes an important additional source to compensate for the demand for the resource, due to the lack of drinking water to satisfy the requirements of the populations at low

costs, with benefits for agricultural soils, taking into account the reduction of the impact on the environment. However, the use of contaminated water in Peru is a risk to the public health, especially when it is used to irrigate crops that are for direct consumption [Larios et al., 2015].

Therefore, the configuration of a system model that allows the effective recovery of gray water by photocatalysis with different times of exposure to solar radiation and differentiated doses of TiO_2 nanoparticles for irrigation of crops was proposed.

MATERIALS AND METHODS

Grey waters

The waters which come from the use of the shower, sink and washing clothes are soapy. Gray water differs from black water because it does not contain fecal bacteria, such as *Escherichia coli* (E-Coli) [Ofori et al., 2021]. Therefore, with proper treatment, they can be used to irrigate plants, promoting agriculture and the sustainability of water use.

Solar radiation on the Earth's surface

The irradiance that reaches the upper atmosphere of the Earth is defined as a solar constant, having the value established by NASA [2010] 1,361 W/m^2 and 1,373 W/m^2 according to the World Meteorological Organization (WMO) [Roldán, 2012]. Solar radiation on the earth's surface is affected by geographic parameters, atmospheric composition, cloudiness, among others, which determine its nature and value. The spectral distribution of solar radiation emitted by a black body at a temperature of 5,900 °K, in the upper part of the atmosphere contains the three distributed radiation regions; 7.20% ultraviolet, 47.20% visible light and 45.60% infrared [Coulson, 1975].

Ultraviolet solar radiation

The solar radiation is made up of different types of radiation, mainly the ultraviolet that ranges up to 400 nm, the visible ranges from 400 to 780 nm and the infrared over 780 nm [Duffie & Beckman, 2020].

The index ultraviolet radiation (IUV) indicates the irradiance per variation of wavelength

in the range of 280 to 400 nm by a constant k_{er} , as seen in equation (1) [Madronich, 2007, p. 1537].

$$IUV = k_{er} \int_{280}^{400} I(\lambda)\varepsilon(\lambda)d\lambda \quad (1)$$

where: $I(\lambda)$ represents the global solar irradiance at surface level for λ ,

k_{er} has a value of 40 m²/W,

$\varepsilon(\lambda)$ is the erythemic action coefficient is represented by:

$$\lambda < 298 \text{ nm} \rightarrow \varepsilon(\lambda)$$

$$328 \text{ nm} < \lambda < 298 \text{ nm} \rightarrow \varepsilon(\lambda) = 10^{0.094 \times (298 - \lambda \times 1000)}$$

$$400 \text{ nm} < \lambda < 328 \text{ nm} \rightarrow \varepsilon(\lambda) = 10^{0.015 \times (139 - \lambda \times 1000)}$$

Considering the dependence of the ozone concentration, the IUV is expressed as in equation (2) [Madronich, 2007, p. 1538].

$$IUV \sim 12.5(\mu_0)^{2.42} \left(\frac{\Omega}{300}\right)^{-1.23} \quad (2)$$

where: μ_0 is represented by the cosine of the azimuthal angle,

Ω represents the total ozone.

The the average daily UV radiation indices for the month with the lowest solar radiation without the presence of a cloud for the solar noon in the city of Pampas where the research work is carried out, exceed the value 10. Zaratti et al. [2014] mentions that just under 90% of the world’s population is exposed to the UV radiation with indices that exceed 10, and in the areas close to the equator, as is the case in the study area, in the months of high solar radiation, this index exceeds 20.

Solar photocatalyst

A solar photocatalyst is the one that captures UV solar radiation and affects the reactor where

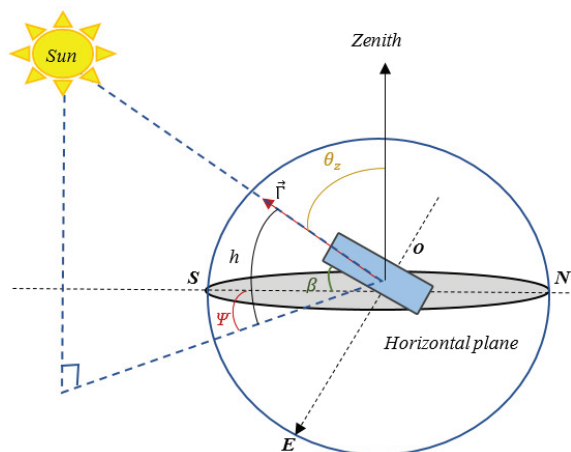


Figure 1. Photoreactor inclination angle

the chemical reactions take place. It is also considered a kind of solar collector; these solar collectors can be mobile or static. For the study, the photocatalyst is static; therefore, it is considered as a flat plate oriented towards the equator with an elevation angle of the latitude of the place (-12.395178°) multiplied by the factor 0.87 (for being in the southern hemisphere), which is recommended for the greater capture of sunlight as a result of solar UV radiation [Nfaoui & El-Hami, 2018], so the UV solar photocatalyst will be oriented to the north with an elevation angle of approximately $\beta = 11^\circ$ (Figure 1).

The photocatalyst implemented uses a tube with composite parabolic cylindrical radiation reflectors (CPC) in a static system, being an economical and efficient option for photochemical processes. [Otálvaro et al., 2017], the CPC has a highly reflective surface that generates a radiative envelope around the cylindrical reactor. In this type of reactors, the concentration factor (CF) is close to 1 when the position is perpendicular to solar radiation, which constitutes one of the advantages of this kind of static system.

Titanium dioxide

Titanium dioxide (TiO₂) is used in the photocatalytic process, because it has high quantum yields, and it is the one that gives high degradation capacity [Hashimoto et al., 2005]. The TiO₂ particle illuminated by sunlight generates photocatalysis due to UV radiation with wavelengths in the range of $280 \leq \lambda \leq 400$, with a photon energy equal to 3.2 electron-volt ($E = 3.2 \text{ eV}$), allowing the passage of one electron from the valence band until reaching the conduction band (Figure 2) generating radicals in the presence of contaminated water OH^{*}.

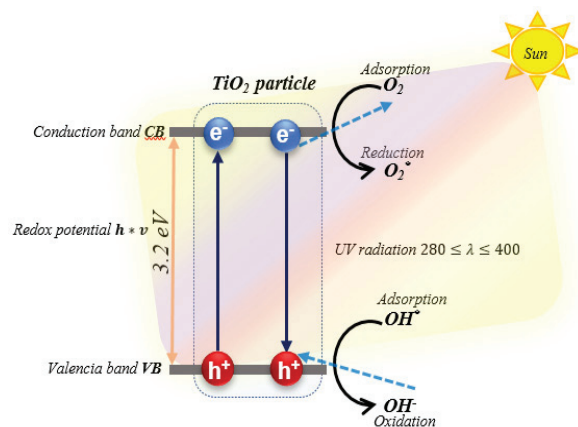


Figure 2. Behavior of a TiO₂ particle in water by action of UV radiation

Titanium dioxide, when analyzed by UV-Visible-IR spectroscopy, presents the absorbance spectrum of the anatase type [Mota et al., 2018], with an absorbance around 280 nm, within the UV spectrum.

The methodological development of the work includes the following phases; modeling and implementation of the photocatalyst and design of experiments for the effective recovery of gray water for crop irrigation.

Photocatalyst modeling

The mathematical modeling of the photocatalyst composed of a tubular reactor with a composite parabolic collector of Figure 3 was carried out taking into account the reference *S* point through the parameters: θ angle equation (3), and ρ the distance equation (4), which traces a line tangent to the tubular reactor [Kreider, 1979].

$$\theta = \overline{OA} \sphericalangle \overline{OR} \quad (3)$$

$$\rho = \overline{RS} \quad (4)$$

In Figure 3, there are two parts that allow establishing a mathematical expression for the incidence of radiation on the cylinder, one is the section AB and the other is BC, for which equations (5 and 6) are established.

For section AB of the curve;

$$\rho = r\theta; |\theta| \leq \theta_a + \pi/2 \quad (5)$$

For section BC of the curve;

$$\rho = r \frac{\theta + \theta_a + \pi - \cos(\theta - \theta_a)}{1 + \sin(\theta - \theta_a)} ; \quad (6)$$

$$\theta_a + \pi/2 \leq |\theta| \leq \frac{3\pi}{2} - \theta_a$$

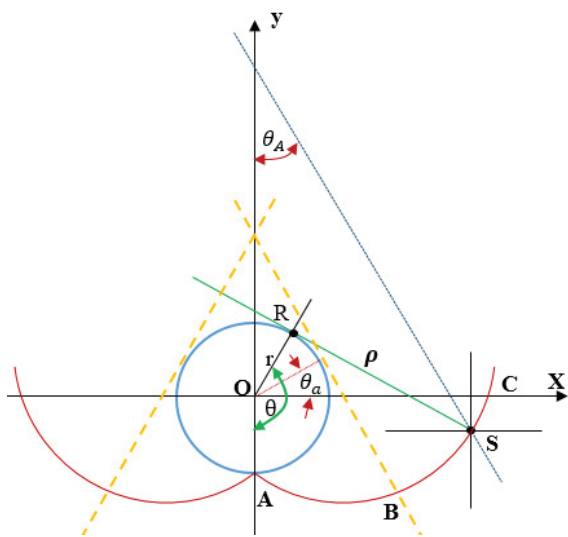


Figure 3. CPC collector radiation curve

The inverse of the sine of the θ_a angle equation (7) is known as the factor that allows the concentration of a CPC collector (C_{CPC}):

$$C_{CPC} = \frac{1}{\sin\theta_a} \quad (7)$$

The concentration factor ranges from 1 to 1.15, since the acceptance angle (θ_a) varies from 60° to 90°. The CPC collector in Figure 4 has as a reflector element the material composed of aluminum and zinc, and the photoreactor tubes are made of high transparency borosilicate glass.

Implementation of the photocatalyst

The process for the photocatalyst, as shown in Figure 5, begins with the provision of gray water to a main process tank, where the mixture of the different doses of TiO_2 is carried out according to the design of the experiment. The water parameters (pH, EC, DO, Turbidity, ORP, FCL) and the solar UV radiation index (IUUV) are measured online from the S7 1500 PLC (Programmable Logic Controller) and the 8X AI U/I/RTD/TC ST analog input module [Siemens, 2014]. The data is normalized and scaled according to the characteristics of the sensors, using the Norm_X and Scale_X functions in the Step 7 software of the TIA Portal; these values are stored in a database that can be exported to a Microsoft Excel spreadsheet.

The gray water is transferred to the photoreactor where it is exposed to solar UV radiation for different periods of time, programmable from an interface for the S7 1500 PLC. Once the exposure period has concluded, the treated water returns to the main process tank for a new reading and storage of water parameter values. The execution of the experiment is then completed and the treated water is automatically moved through a filter to the final storage tank.

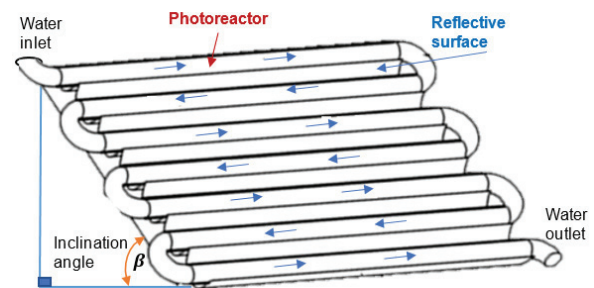


Figure 4. CPC collector scheme for the photocatalytic process

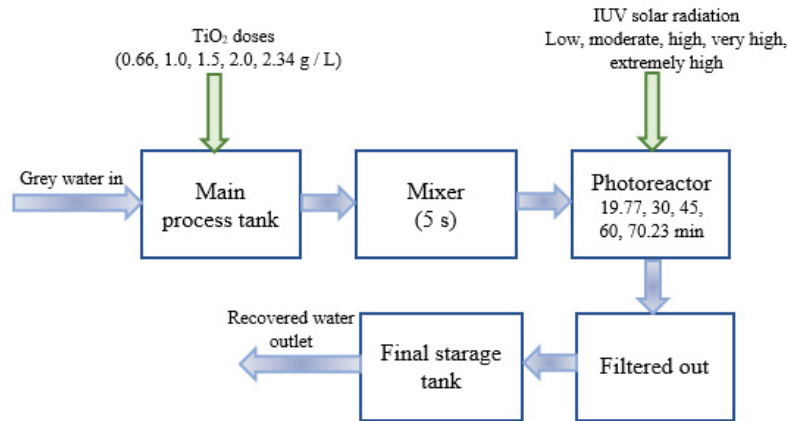


Figure 5. Flow chart of the implemented photocatalyst operation

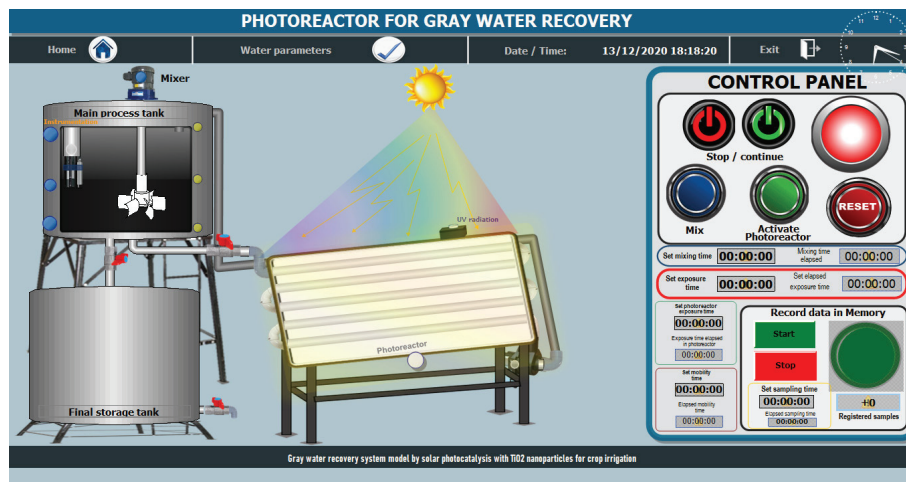


Figure 6. HMI interface of the photoreactor for gray water recovery

The HMI interface of the photoreactor of Figure 6 is connected to the S7 1500 PLC, where the main process tank initially stores the gray water to be treated. In the photoreactor the exposure to solar UV radiation of the water under treatment is monitored, the control panel allows automatically stopping or continuing the process, mixing the gray water with the TiO_2 , activating the photoreactor and restarting the process, it also allows establishing the period of exposure of the water in treatment to solar UV radiation, as well as to activate the recording of measured parameter values on a database.

Design of experiments

The context was constructed and the independent variables were intentionally manipulated to evaluate the study variables. In order to achieve the objectives, the authors worked with data that characterize the variables from the experimental tests and the analysis of parameters of greywater.

The data was obtained automatically from the gray water parameter sensors. The data collection instruments were previously calibrated for the measurement of the 6 water parameters (pH, EC, DO, Turbidity, ORP and FCL).

The central compound design was applied, with 3 factors at its levels: high, medium and low (1, 0, -1); the same one that has 6 central points and 6 axial points, with 20 observations and runs. This type of design is the most efficient for the analysis of the data with the response surfaces methodology [Melo et al., 2020]. Process variables are encoded as x_1, x_2, x_3 being $x_1 = \frac{\xi_1 - 8.5}{4.5}$, $x_2 = \frac{\xi_2 - 1.5}{0.5}$, $x_3 = \frac{\xi_3 - 45.5}{15}$; ξ_1 denotes the natural variable to the IUV, ξ_2 represents the natural variable TiO_2 , and ξ_3 the natural variable time.

The axial points were calculated with 2^k , where $k = 3$ is the number of factors, so the number of factors is $2^3 = 8$. The distance to which the axial points should be placed is calculated with $\alpha = (2^k)^{1/4}$, getting $\alpha = \pm 1.68$.

The response surface analysis was made for the model of second order, according to the following expression of equation 8.

$$\hat{y} = b_0 + \sum_{i=1}^k b_i x_i + \sum_{i=1}^k b_{ii} x_i^2 + \sum_{i=1}^k \sum_{j=1}^k b_{ij} x_i x_j, i < j \tag{8}$$

RESULTS

Water quality obtained

With the implemented system and previously calibrated sensor-transducers for the reliable measurement of water parameters [Vargas & González, 2014], 20 different experiments were carried out according to the central compound design, with six central points and six established axial points, obtaining the data described in Table 1.

The analysis of variance (ANOVA) of three factors was applied to the result obtained in Table 1, being the level of significance. In Table 2, the coded coefficients are obtained $\alpha = 0.05$.

Table 3 presents the analysis of variance for the linear, quadratic, and quadratic models with interaction of factors.

The response surface analysis of the various interactions of the variables involved in the complete quadratic equation is shown in Figures 7, 8 and 9.

Factor optimization of the gray water recovery model

The factors (IUV, TiO₂ and exposure time) were optimized within the ranges experienced, using Minitab V19, restricting the IUV levels (4 to 13), with TiO₂ (1 to 2 g/L) and the time of unrestricted exposure, with the objective of obtaining recovered gray water with a quality equal to or greater than 90% (Table 4), the water being without threats and with conditions close to the desired levels, with a confidence level of 95%.

The results were analyzed to achieve the objective, reaching the following:

- a) The intervention of solar UV radiation in the gray water recovery process is of great importance, the greater UV radiation, the shorter the photoreaction, which is evidenced in the results of the experiment in Table 1 (Obs10) reaching water with a quality index of 86.34%
- b) The applied doses of nanoparticles of TiO₂ ranged from 0.6591 g/L to 2.34 g/L, obtaining

Table 1. Water quality index obtained for the six central points and six axial points of the experiment design

Observation	Run order	Process variables			Coded variables			Water quality index (ICA-PE)
		UV radiation	TiO ₂ (g/L)	Time (min)	x ₁	x ₂	x ₃	Y
Obs1	1	4	1.0	30	-1	-1	-1	34.98
Obs2	2	13	1.0	30	1	-1	-1	55.63
Obs3	3	4	2.0	30	-1	1	-1	39.31
Obs4	4	13	2.0	30	1	1	-1	86.21
Obs5	5	4	1.0	60	-1	-1	1	38.40
Obs6	6	13	1.0	60	1	-1	1	86.34
Obs7	7	4	2.0	60	-1	1	1	56.49
Obs8	8	13	2.0	60	1	1	1	86.35
Obs9	9	0.93	1.5	45	-1.68	0	0	34.10
Obs10	10	16.07	1.5	45	1.68	0	0	86.30
Obs11	11	8.5	0.66	45	0	-1.68	0	51.18
Obs12	12	8.5	2.34	45	0	1.68	0	72.61
Obs13	13	8.5	1.5	19.77	0	0	-1.68	47.42
Obs14	14	8.5	1.5	70.23	0	0	1.68	86.39
Obs15	15	8.5	1.5	45	0	0	0	56.40
Obs16	16	8.5	1.5	45	0	0	0	56.50
Obs17	17	8.5	1.5	45	0	0	0	56.51
Obs18	18	8.5	1.5	45	0	0	0	56.37
Obs19	19	8.5	1.5	45	0	0	0	56.56
Obs20	20	8.5	1.5	45	0	0	0	56.55

Table 2. Value of the coded coefficients

Term	Coef	EE of the coef.	T value	P value
Constant	56.58	2.53	22.37	0.000
IUV	17.07	1.68	10.17	0.000
TiO ₂	6.52	1.68	3.89	0.003
Time	8.57	1.68	5.10	0.000
IUV·IUV	0.70	1.63	0.43	0.679
TiO ₂ ·TiO ₂	1.29	1.63	0.79	0.447
Time·Time	3.07	1.63	1.88	0.090
IUV·TiO ₂	1.02	2.19	0.47	0.652
IUV·Time	1.28	2.19	0.58	0.572
TiO ₂ ·Time	-2.10	2.19	-0.96	0.361

Table 3. Variance analysis

Source	GL	SC Adj.	MC Adj.	F value	P value
Model	9	5770.25	641.14	16.67	0.000
Linear	3	5562.45	1854.15	48.21	0.000
IUV	1	3979.87	3979.87	103.48	0.000
TiO ₂	1	580.72	580.72	15.10	0.003
Time	1	1001.86	1001.86	26.05	0.000
Square	3	151.01	50.34	1.31	0.325
IUV·IUV	1	6.97	6.97	0.18	0.679
TiO ₂ ·TiO ₂	1	24.14	24.14	0.63	0.447
Time·Time	1	135.41	135.41	3.52	0.090
Interaction of 2 factors	3	56.80	18.93	0.49	0.696
IUV·TiO ₂	1	8.34	8.34	0.22	0.652
IUV·Time	1	13.16	13.16	0.34	0.572
TiO ₂ ·Time	1	35.31	35.31	0.92	0.361
Error	10	384.62	38.46	–	–
Lack of fit	5	384.59	76.92	12972.29	0.000
Pure error	5	0.03	0.01		
Total	19	6154.87			

Table 4. Value of factors that optimize greywater recovery

Solution	IUV	TiO ₂ (g / L)	Weather (min)	ICA Adjustment	Compound desirability
1	12.21	1,973	60,041	90.00	1.00

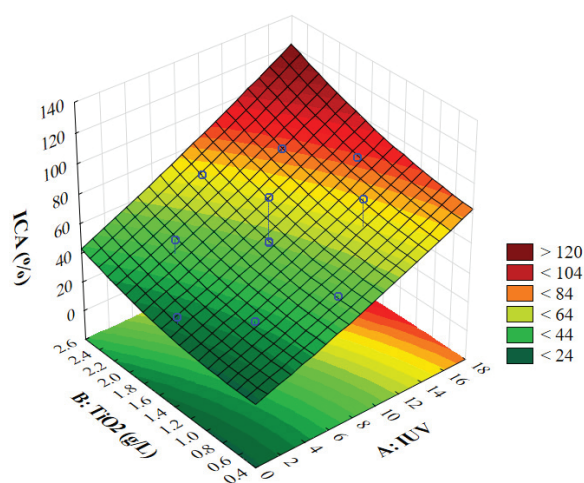


Figure 7. Response surface of the IUV – TiO₂ interaction

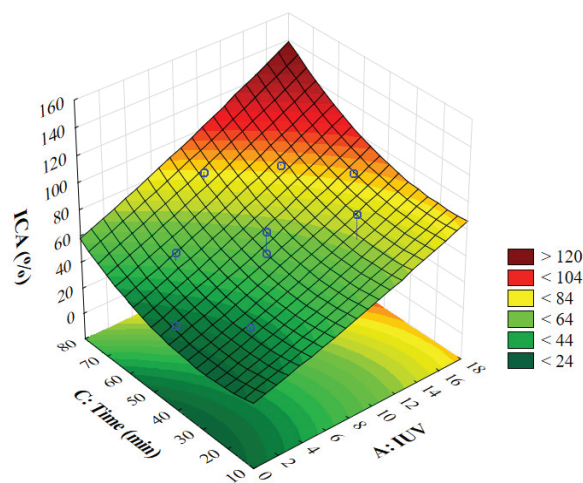


Figure 8. Response surface for IUV interaction – Exposure time

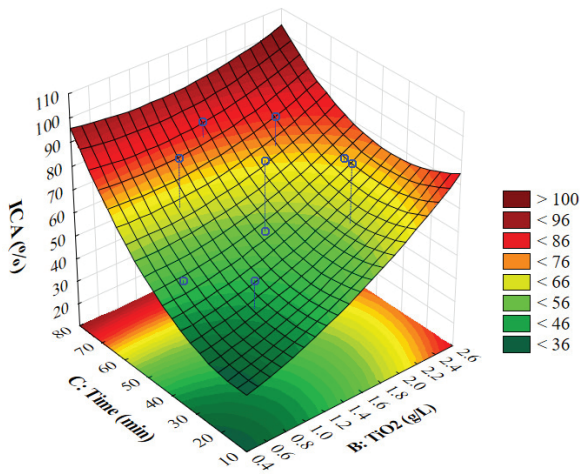


Figure 9. Response surface for TiO₂ interaction – Exposure time

the best results with respect to this factor in experiment 8 (Obs8) of Table 1, where it allows obtaining the water with a quality index 86.35, the dose being 2.0 g/L, with an IUUV 13 and an exposure time of 60 minutes.

- c) The period of exposure of the water in treatment had an interval of 19.77 to 70.23 minutes, obtaining better results with respect to this factor in experiment 14 (Obs14) for an IUUV of 8.5, and a TiO₂ dose of 1.5 g/L.
- d) In order to determine the mathematical behavior of the gray water recovery process represented by the water quality index (%), which is the response variable (and), first and second order mathematical models were evaluated, being the one that best adjusted that of second order indicated in equation (9):

$$y = 14.9 + 1.67x_1 + 6.3x_2 - 0.396x_3 + 0.0344x_1^2 + 5.18x_2^2 + 0.01362x_3^2 + 0.454x_1 \cdot x_2 + 0.019x_1 \cdot x_3 - 0.28x_2 \cdot x_3 \quad (9)$$

DISCUSSION AND CONCLUSIONS

On the quality of water obtained

Solar UV radiation is a key factor for photocatalytic processes, in the results of this work it has been evidenced in experiments, especially in observation 10 of Table 1. UV radiation, upon reaching a parabolic surface, has a higher concentration and manages to cross the glass tube of the photoreactor, generating reactions with photosensitive elements, such as TiO₂. Another favorable aspect was located in the central area of Peru,

where the UV radiation index exceeds 10 in times of lesser solar radiation, rising to more than 20 in times of greater radiation, due to the fact that the Earth is closer to the Sun, turning this radiation into a sustainable resource Zaratti et al. [2014]. This finding agrees with other studies: Ponce [2018], in the results of the study of wastewater treatment through processes that use solar radiation and ozone, established that the photo-fenton solar processes require a high and stable IUUV to achieve the mineralization of pollutants.

Castro [2017] used solar radiation to deactivate the bacteria in water in PET bottles, finding a mathematical model with parameters obtained by regression, achieving an intracellular attack as a consequence of the action of photons from sunlight. Moreover, Barwal and Chaudhary [2016], in a study for municipal water treatment, developed a parabolic concentrator to take advantage of solar energy, improving from 400 to 700 W/m² in full Sun and from 170 to 250 W/m² on cloudy days, which resulted in an increase efficiency of 40% and 13% respectively.

The TiO₂ dose of 2.0 g/L, IUUV 13 and an exposure time of 60 minutes, water is obtained with a quality index of 86.35%, to avoid sedimentation, this semiconductor was dissolved in the photoreactor and mobilized with displacements in short times by means of a recirculating water pump programmable from a human machine interface screen and maintaining kinetic efficiency. This, in order to take advantage of the photocatalytic properties of TiO₂, since it is a semiconductor that, when illuminated by sunlight, generates photocatalysis due to UV radiation, with water acting as a donor and acceptor of electrons so that in the process produces oxidation – causes a reduction of pollutants [Plantard et al., 2021]. Mobility is necessary for the photocatalytic action of TiO₂ to be able to prolong its usefulness, as reported by Jiménez [2015]. TiO₂ can be combined with other elements to improve the photo degradation efficiency in specific applications [Zawadzki et al., 2020].

On the other hand, Borges et al. [2016], in the research they carried out, concluded that the photocatalytic process represents a sustainable alternative, achieving the degradation of 95% of the contaminated water after 2 hours, and high oxidative capacity of this system. Moreover, Powell, Litter, Blesa and Apella [2007], in the research carried out, determined that both solar disinfection (SODIS) and hybrid photocatalytic

disinfection (FHS) offer bacterial removal at acceptable levels, the requirement being 4 hours of exposure to the Sun in spring, summer and autumn. The changes in the initial values of pH, conductivity, dissolved oxygen and bacterial concentration did not determine the efficiency of the disinfection process. Therefore, it was necessary to apply a combined treatment with TiO₂.

From the optimization of factors of the gray water recovery model

The mathematical model determines the behavior of the gray water recovery process; from the result, this model represents the water quality index (%) which is the response variable “y”. The linear model, quadratic linear model, and complete quadratic model were evaluated. Determination of the latter model describes the recovery of chalk waters with the highest determination index ($R^2 = 91.86$) for $\alpha = 0.05$

Finally, it can be indicated that the factors involved in the recovery of gray water are correlated. Therefore, when optimizing water quality to 90% according to ICA-PE, the configuration of the system model has a solar UV index of 12.21, TiO₂ nanoparticles dissolved in a dose of 1.973 g/L and with a period of solar exposure of 60.04 minutes in the photocatalyst that was implemented for this purpose, having the particularity of being programmable and keeping the treatment water in motion to avoid sedimentation.

Acknowledgements

I appreciate the support obtained from the Facultad de Ingeniería Electrónica-Sistemas, of the Universidad Nacional de Huancavelica, for the support with equipment and instruments for the implementation of the gray water recovery system.

REFERENCES

1. Adrados, B., Sánchez, O., Arias, C.A., Becares, E., Garrido, L., Mas, J., Brix, H., & Morató, J. 2014. Microbial communities from different types of natural wastewater treatment systems: Vertical and horizontal flow constructed wetlands and bio-filters. *Water Research*, 55, 304–312. <https://doi.org/10.1016/j.watres.2014.02.011>
2. Almomani, F., Bhosale, R., Kumar, A., & Khraisheh, M. 2018. Potential use of solar photocatalytic oxidation in removing emerging pharmaceuticals from

- wastewater: A pilot plant study. *Solar Energy*. <https://doi.org/10.1016/J.SOLENER.2018.07.041>
3. Barwal, A., & Chaudhary, R. 2016. Feasibility study for the treatment of municipal wastewater by using a hybrid bio-solar process. *Journal of Environmental Management*, 177, 271–277. <https://doi.org/10.1016/J.JENVMAN.2016.04.022>
4. Borges, M.E., Sierra, M., Cuevas, E., García, R.D., & Esparza, P. 2016. Photocatalysis with solar energy: Sunlight-responsive photocatalyst based on TiO₂ loaded on a natural material for wastewater treatment. *Solar Energy*, 135, 527–535. <https://doi.org/10.1016/J.SOLENER.2016.06.022>
5. Casadei, E., & Albert, J. 2016. Food and Agriculture Organization of the United Nations. *Encyclopedia of Food and Health*, 749–753. <https://doi.org/10.1016/B978-0-12-384947-2.00270-1>
6. Castro, M. 2017. Modelado cinético de la inactivación de escherichia coli en agua mediante radiación solar y aplicaciones de sodis [tesis de doctorado, Universidad de Almería]. <https://dialnet.unirioja.es/servlet/tesis?codigo=181541&orden=0&info=link>
7. Coulson, K. 1975. Solar and terrestrial radiation: methods and measurements. In *Physics Bulletin*. Academic Press. <https://doi.org/10.1002/9781119540328>
8. Deza Martí, E., Osorio Anaya, A., & Manrique Fajardo, J.J. 2017. Evaluación experimental de la degradación fotocatalítica del colorante Cibacron Navy H-2G empleando nanopartículas industriales de TiO₂. *Revista de La Sociedad Química Del Perú*, 83(2), 160–173. <https://doi.org/10.37761/rsqp.v83i2.193>
9. Duffie, J.A., & Beckman, W.A. 2020. *Solar engineering of thermal processes, photovoltaics and wind* (5th ed.). Wiley. <https://doi.org/10.1002/9781119540328>
10. Hashimoto, K., Irei, H., & Fijishima, A. 2005. TiO₂ Photocatalysis: A Historical Overview and Future Prospects. *Japanese Journal of Applied Physics*. <https://doi.org/10.1143/JJAP.44.8269>
11. Jeppesen, B. 1996. Domestic greywater reuse: Australia’s challenge for the future. *Desalination*, 311–315. [https://doi.org/10.1016/S0011-9164\(96\)00124-5](https://doi.org/10.1016/S0011-9164(96)00124-5)
12. Jiménez, M. 2015. Desarrollo de nuevas estrategias basadas en fotocatalisis solar para la regeneración de aguas de una industria agro-alimentaria [tesis de doctorado, Universidad de Almería]. https://www.psa.es/es/areas/tsa/docs/Tesis_Margarita_Jimenez.pdf
13. Kamizoulis, G. 2008. Setting health based targets for water reuse (in agriculture). *Desalination*, 218(1–3), 154–163. <https://doi.org/10.1016/j.desal.2006.08.026>
14. Kreider, J.F. 1979. Medium temperature solar collectors and ancillary components. In *Academic Press* (pp. 100–160). <https://doi.org/10.1016/b978-0-12-425980-5.50009-1>.

15. Larios, J.F., Gonzales, C., & Morales, Y. 2015. Las aguas residuales y sus consecuencias en el Perú. *Revista de La Facultad de Ingeniería de La USIL*. [https://doi.org/10.1016/S0011-9164\(96\)00124-5](https://doi.org/10.1016/S0011-9164(96)00124-5)
16. Madronich, S. 2007. Analytic formula for the clear-sky UV index. *Photochemistry and Photobiology*, 83(6), 1537–1538. <https://doi.org/10.1111/j.1751-1097.2007.00200.x>
17. Melo, O.O., López, L.A., & Melo, S.E. 2020. *Diseño de experimentos: Métodos y aplicaciones (2nd ed.)*. Universidad Nacional de Colombia.
18. Mohamed, R.M.S.R., Kassim, A.H.M., Anda, M., & Dallas, S. 2013. A monitoring of environmental effects from household greywater reuse for garden irrigation. *Environmental Monitoring and Assessment*, 185(10), 8473–8488. <https://doi.org/10.1007/s10661-013-3189-0>
19. Mota, M., Hernández, H., & Alaniz, M. 2018. TiO₂ obtenido por el proceso sol gel asistido con microondas. *Latin American Journal of Applied Engineering*, 3(1), 1–4. <http://lajae.uabc.mx/index.php/journal/article/view/97/75>
20. NASA, 2010. Observatorio de dinámica solar: La misión del “Sol variable.” https://ciencia.nasa.gov/science-at-nasa/2010/05feb_sdo
21. Nfaoui, M., & El-Hami, K. 2018. Extracting the maximum energy from solar panels. *Energy Reports*, 4, 536–545. <https://doi.org/10.1016/j.egy.2018.05.002>
22. Ofori, S., Puškáčková, A., Růžičková, I., & Wanner, J. 2021. Treated wastewater reuse for irrigation: Pros and cons. *Science of The Total Environment*, 760, 144026. <https://doi.org/https://doi.org/10.1016/j.scitotenv.2020.144026>
23. Otálvaro, H.L., Mueses, M.A., Crittenden, J.C., & Machuca, F. 2017. Solar photoreactor design by the photon path length and optimization of the radiant field in a TiO₂-based CPC reactor. *Chemical Engineering Journal*, 315, 283–295. <https://doi.org/10.1016/j.cej.2017.01.019>
24. Plantard, G., Dezani, C., Ribeiro, E., Reoyo-Prats, B., & Goetz, V. 2021. Modelling heterogeneous photocatalytic oxidation using suspended TiO₂ in a photoreactor working in continuous mode: Application to dynamic irradiation conditions simulating typical days in July and February. *Canadian Journal of Chemical Engineering*, 99(1), 142–152. <https://doi.org/10.1002/cjce.23870>
25. Ponce, L. 2018. *Tratamiento de aguas residuales mediante procesos basados en la radiación solar y el ozono. Evaluación mediante técnicas analíticas y microbiológicas avanzadas [tesis de doctorado, Universidad de Almería]*. https://www.psa.es/es/areas/tsa/docs/Tesis_Laura_Ponce.pdf
26. Powell, P. A., Litter, M., Blesa, M.A., & Apella, M. C. 2007. Desinfección solar de aguas por fotólisis y fotocatalisis: aplicación en Tucuman, Argentina. *Medioambiente En Iberoamérica*, 2, 1–6. <https://dialnet.unirioja.es/servlet/articulo?codigo=7397894>
27. Roldán, J. 2012. *Estudios de viabilidad de instalaciones solares*. Paraninfo.
28. Siemens, 2014. Analog input module AI 8xU/I/RTD/TC ST (6ES7531-7KF00-0AB0) Manual. https://cache.industry.siemens.com/dl/files/205/59193205/att_112065/v1/s71500_ai_8xu_i_rtd_tc_st_manual_en-US_en-US.pdf
29. Silva, J., Torres, P., & Madera, C. 2008. Reuso de aguas residuales domésticas en agricultura. Una revisión. *Agronomía Colombiana*, 26(2), 347–359. https://www.researchgate.net/publication/262458195_Reuso_de_aguas_residuales_domesticas_en_agricultura_Una_revisión_Domestic_wastewater_reuse_in_agriculture_A_review
30. UNESCO, 2006. *El Agua: una responsabilidad compartida, 2º informe de las Naciones Unidas sobre el desarrollo de los recursos hídricos en el mundo, resumen ejecutivo*. 52. https://unesdoc.unesco.org/ark:/48223/pf0000144409_spa
31. Vargas, G., & González, G. 2014. Calibración de medidores de pH: una visión diferente. *Boletín Científico Técnico INIMET*, 1.
32. Zaratti, F., Piacentini, R.D., Guillén, H.A., Cabrera, S.H., Liley, J. Ben, & McKenzie, R.L. 2014. Proposal for a modification of the UVI risk scale. *Photochemical and Photobiological Sciences*, 13(7), 980–985. <https://doi.org/10.1039/c4pp00006d>
33. Zawadzki, P., Kudlek, E., & Dudziak, M. 2020. Titanium (IV) oxide modified with activated carbon and ultrasounds for caffeine photodegradation: adsorption isotherm and kinetics study. *Journal of Ecological Engineering*, 21(8), 137–145. <https://doi.org/10.12911/22998993/126985>